THE JOURNAL OF BIOLOGICAL CHEMISTRY VOL. 286, NO. 17, pp. 14795–14803, April 29, 2011

Selective Activation of the Transcription Factor NFAT1 by Calcium Microdomains near Ca^{2+} Release-activated Ca^{2+} (CRAC) Channels*[S]

Received for publication, January 11, 2011, and in revised form, February 14, 2011 Published, JBC Papers in Press, February 16, 2011, DOI 10.1074/jbc.M111.220582

Pulak Kar, Charmaine Nelson, and Anant B. Parekh[1]

From the Department of Physiology, Oxford University, Sherrington Building, Parks Road, Oxford OX1 3PT, United Kingdom

NFATs are a family of Ca^{2+}-dependent transcription factors that play a central role in the morphogenesis, development, and physiological activities of numerous distinct cell types and organ systems. Here, we visualize NFAT1 movement in and out of the nucleus in response to transient activation of store-operated Ca^{2+} release-activated Ca^{2+} (CRAC) channels in nonexcitable cells. We show that NFAT migration is exquisitely sensitive to Ca^{2+} microdomains near open CRAC channels. Another Ca^{2+}-permeable ion channel (TRPC3) was ineffective in driving NFAT1 to the nucleus. NFAT1 movement is temporally dissociated from the time course of the Ca^{2+} signal and remains within the nucleus for 10 times longer than the duration of the trigger Ca^{2+} signal. Kinetic analyses of each step linking CRAC channel activation to NFAT1 nuclear residency reveals that the rate-limiting step is transcription factor exit from the nucleus. The slow deactivation of NFAT provides a mechanism whereby Ca^{2+}-dependent responses can be sustained despite the termination of the initial Ca^{2+} signal and helps explain how gene expression in nonexcitable cells can continue after the primary stimulus has been removed.

Cytoplasmic Ca^{2+} is a universal signal that activates a myriad of spatially and temporally distinct cellular responses (1). Intrinsic to the use of such a multifarious intracellular messenger is the question of specificity. How can selective responses be induced by a signal capable of influencing numerous cellular activities simultaneously? It has now been firmly established that spatially restricted local Ca^{2+} signals (Ca^{2+} microdomains) provide a rapid, robust, and reliable route for selective activation of co-localized targets (2, 3). Well understood examples utilizing Ca^{2+} microdomains include the tight functional coupling between voltage-gated Ca^{2+} channels and the rapidly releasable pool of secretory vesicles in presynaptic nerve terminals (2) and between inositol trisphosphate-sensitive Ca^{2+} channels in the endoplasmic reticulum and the uniporter Ca^{2+} channels in the mitochondrial inner membrane (4). A more complex scenario arises when the target is located at a considerable distance from the realm of the local Ca^{2+} signal, as illustrated by stimulus-transcription coupling. Here, local Ca^{2+} signals accompanying the opening of either voltage-gated Ca^{2+} channels or store-operated CRAC[2] channels in the plasma membrane activate Ca^{2+}-dependent gene expression in the nucleus (5–7). This form of signaling is remarkable in two ways. First, the local Ca^{2+} signal extends just a few nanometers from the channel pore yet influences events located several micrometers away (3). Second, a burst of channel activity for just a few seconds to minutes leads to gene expression several hours later (7). Hence, the impact of the Ca^{2+} microdomain is expanded over several orders of magnitude in both the spatial and temporal domains.

One well studied Ca^{2+}-dependent transcription factor is the nuclear factor of activated T cells (NFAT). Four members of the NFAT family (NFAT1–4) are stimulated by a rise in cytoplasmic Ca^{2+}, and activated NFAT regulates numerous inducible genes that are essential for synaptic plasticity, axonal growth, and neuronal survival (8, 9) as well as T cell development and the generation of effective immune responses (10). The Ca^{2+} rise required for NFAT activation occurs through the opening of voltage-gated L-type Ca^{2+} channels in hippocampal neurons (8) and CRAC channels in the plasma membrane of nonexcitable cells (11, 12). In both cases, Ca^{2+} influx leads to stimulation of the Ca^{2+}-calmodulin-dependent protein phosphatase calcineurin, which dephosphorylates multiple residues on cytosolic NFAT (13, 14). This exposes a nuclear localization sequence, resulting in NFAT import to the nucleus. Nuclear confined NFAT leads to gene expression, often in tandem with the AP-1 transcription factor complex of c-Fos and c-Jun (10). An essential role for CRAC channels in activation of NFAT in T cells has been established from studies on patients with a single point mutation (R91W) in the pore-forming Orai1 subunit (15). The R91W mutant CRAC channel fails to conduct Ca^{2+}, and NFAT activation is suppressed.

In cultured hippocampal neurons, several pieces of evidence suggest that Ca^{2+} microdomains near the L-type Ca^{2+} channels selectively couple to NFAT activation. First, depolarization with high K^+ solution triggers NFAT migration to the nucleus, and despite the presence of other types of voltage-gated Ca^{2+} channel, this is prevented by L-type channel blockers (8, 9). Second, loading the cytoplasm with the slow Ca^{2+} chelator EGTA fails to impede NFAT movement (9). Third, calcineurin is tethered next to L-type channels through the anchoring protein AKAP79/150 (9). Despite the fundamental importance of

* This work was supported by the Medical Research Council (United Kingdom) and the British Heart Foundation Centre of Excellence award.

[S] The on-line version of this article (available at http://www.jbc.org) contains supplemental Fig. 1.

[1] To whom correspondence should be addressed. Tel.: 44-1865-282174; Fax: 44-1865-272488; E-mail: anant.parekh@dpag.ox.ac.uk.

[2] The abbreviations used are: CRAC, Ca^{2+} release-activated Ca^{2+}; NFAT, nuclear factor of activated T cells; OAG, 1-oleoyl-2-acetyl-*sn*-glycerol.

the Ca^{2+}-NFAT interaction to nonexcitable cells, several questions remain. Is NFAT activated by Ca^{2+} microdomains near CRAC channels or is a bulk rise in cytoplasmic Ca^{2+} sufficient? If Ca^{2+} acts locally, how local is local? How rapidly does NFAT migrate in and out of the nucleus? Using an NFAT1 construct tagged with GFP, we have addressed these issues using high resolution single cell live imaging. We find that NFAT1 activation is tightly coupled to Ca^{2+} microdomains near open CRAC channels. We find evidence for strong short term memory in that NFAT1 movement into the nucleus outlasts the cytoplasmic Ca^{2+} signal by several minutes. Our results also reveal that NFAT1 exits from the nucleus slowly and long after the Ca^{2+} signal has been terminated. This relatively slow deactivation rate of NFAT ensures that a pulse of CRAC channel activity for a few minutes is sufficient to maintain NFAT in the nucleus for considerably longer, thereby promoting gene expression while obviating the detrimental effects of a sustained global Ca^{2+} rise. Long lasting Ca^{2+}-dependent responses can therefore be achieved through the slow deactivation (off rate) of an effector.

MATERIALS AND METHODS

Cell Culture—HEK293 cells were purchased from ATCC (via UK supplier LGC) and were cultured at 37 °C with 5% CO_2 in Dulbecco's modified Eagle's medium (DMEM) supplemented with 10% fetal bovine serum and 1% penicillin/streptomycin. RBL-1 cells were also purchased from ATCC and cultured as described previously (16).

cDNA Constructs and Transfection—NFAT1-GFP was a kind gift from Dr. Paul Worley (The Johns Hopkins School of Medicine). The EGFP-based reporter plasmid (pNFAT-TA-EGFP) was a kind gift from Dr. Yuriy Usachev (University of Iowa). Orai1 was from OriGene, and STIM1-YFP was a generous gift from Dr. Tobias Meyer (Stanford University). HEK293 cells were transfected using the Lipofectamine method. All plasmids were used at 1 μg, and experiments commenced 24–48 h after transfection. Two sources of HEK293 cells stably expressing TRPC3 channels were used, one kindly provided by Dr. James Putney (NIEHS, National Institutes of Health) and the other kindly supplied by Dr. Michael Zhou (Ohio State University).

NFAT1-GFP Movement—NFAT1-GFP levels in the cytosol and nucleus were measured using the IMAGO charge-coupled device camera-based system from TILL Photonics, with a ×100 oil immersion objective (numerical aperture 1.3). Regions of interest of identical size were drawn in the cytosol and nucleus of each cell, and fluorescence was computed. Nuclear localization was confirmed by co-staining with a nuclear dye (DAPI; Fig. 1). Unless otherwise indicated, we calculated the nuclear/cytosolic ratio of NFAT-GFP.

Gene Reporter Assay—24–36 h following transfection with the EGFP-based reporter plasmid that contained an NFAT promoter, cells were stimulated with leukotriene C_4 for 40 min, and the percentage of cells expressing EGFP was measured. Gene expression was defined as fluorescence 3 × S.D. > cell autofluorescence, measured in nontransfected cells. Cells were stimulated in culture medium and maintained in the incubator.

Ca^{2+} Measurements—Cytoplasmic Ca^{2+} imaging experiments were carried out at room temperature using the IMAGO charge-coupled device camera-based system from TILL Photonics, as described previously (17). Cells were alternately excited at 356 and 380 nm (20-ms exposures), and images were acquired every 2 s. Images were analyzed off line using IGOR Pro for Windows. Cells were loaded with Fura-2/AM (1 μM) or Fura-5F/AM (Fig. 4*G*) for 40 min at room temperature in the dark and then washed three times in standard external solution composed of 145 mM NaCl, 2.8 mM KCl, 2 mM $CaCl_2$, 2 mM $MgCl_2$, 10 mM D-glucose, 10 mM HEPES, pH 7.4, with NaOH. Cells were left for 15 min to allow further de-esterification. Ca^{2+}-free solution had the following composition: 145 mM NaCl, 2.8 mM KCl, 2 mM $MgCl_2$, 10 mM D-glucose, 10 mM HEPES, 0.1 mM EGTA, pH 7.4, with NaOH. Ca^{2+} signals are plotted as *R*, which denotes the 356/380 nm ratio.

Western Blotting—Total cell lysates (60 μg) were analyzed by SDS-PAGE on a 10% gel. Membranes were blocked with 5% nonfat dry milk in PBS plus 0.1% Tween 20 (PBST) buffer for 1 h at room temperature (18). Membranes were washed with PBST three times and then incubated with primary Ab for 24 h at 4 °C. Total ERK2 and GFP antibodies were from Santa Cruz Biotechnology and Cell Signaling, respectively, and used at dilutions of 1:5000 (ERK2) and 1:2000 (GFP), respectively. The membranes were then washed with PBST again and incubated with 1:2500 dilutions of peroxidase-linked anti-rabbit IgG from Santa Cruz Biotechnology for 1 h at room temperature. After washing with PBST, the bands were detected by an enhanced chemiluminescence (ECL) plus Western blotting detection system (Amersham Biosciences). Blots were analyzed by UNI-Scan software.

Statistical Analysis—Data are presented as the mean ± S.E. Statistical significance was determined using Student's *t* test, where * denotes $p < 0.05$ and ** denotes $p < 0.01$.

RESULTS

NFAT Accumulates in the Nucleus following Opening of CRAC Channels—We initially investigated whether Ca^{2+} entry through CRAC channels drives NFAT1 movement to the nucleus. Stimulation with the sarco/endoplasmic reticulum Ca^{2+}-ATPase pump inhibitor thapsigargin raises cytoplasmic Ca^{2+} by depleting intracellular Ca^{2+} stores. In the absence of external Ca^{2+}, thapsigargin (2 μM) generated a transient Ca^{2+} rise (Fig. 1*A*; *trace labeled 0 Ca^{2+}*). However, this consistently failed to drive NFAT1 movement into the nucleus for up to 40 min after stimulation (Fig. 1, *B* and *F*). On the other hand, a more prolonged Ca^{2+} rise occurred when thapsigargin was applied in the presence of external Ca^{2+} (Fig. 1*A*), and this was associated with prominent NFAT1 movement into the nucleus (Fig. 1, *C* and *F*). Nuclear migration was confirmed by the strong co-localization between NFAT1-GFP and the nuclear dye DAPI after stimulation with thapsigargin in the presence of external Ca^{2+} (Fig. 1*D*). Hence, Ca^{2+} influx through CRAC channels leads to NFAT1 activation and translocation to the nucleus. Consistent with this, pretreatment with the CRAC channel inhibitor Synta compound (5 μM) (18) suppressed NFAT1 movement in response to thapsigargin stimulation in the presence of external Ca^{2+} (Fig. 1, *E* and *F*). CRAC channels activated NFAT movement through recruitment of calcineurin, because pretreatment with the calcineurin inhibitor cyclosporin A (1 μM; Fig. 1, *E* and *F*) suppressed NFAT1 trans-

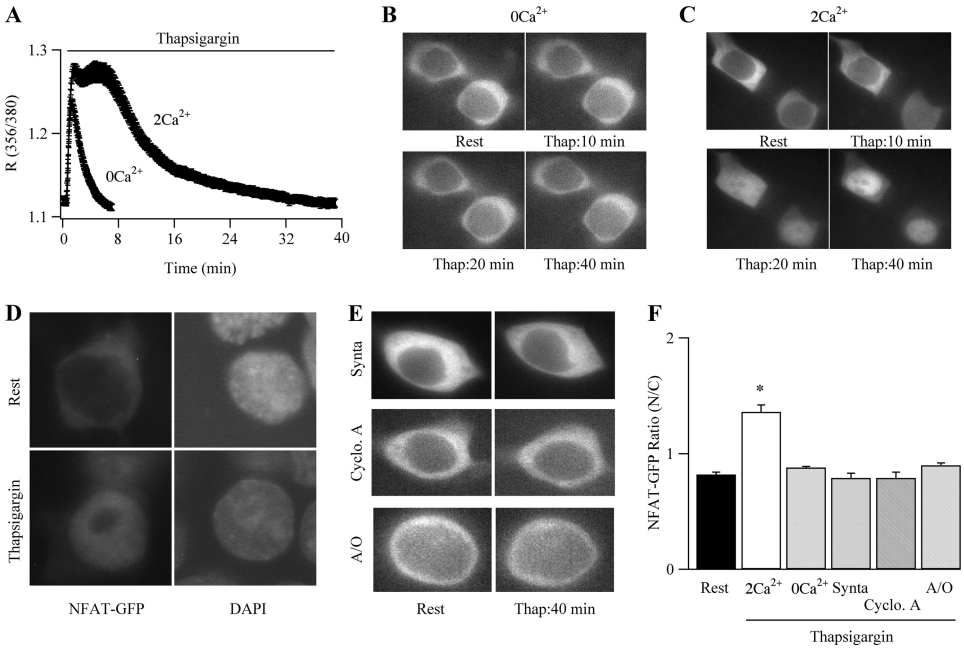

FIGURE 1. **NFAT1 migrates to the nucleus following CRAC channel opening.** *A,* cytoplasmic Ca^{2+} signals to thapsigargin in the presence ($n = 18$ cells) and absence ($n = 21$ cells) of external Ca^{2+}. *B,* NFAT1 movement following store depletion (2 μM thapsigargin) in Ca^{2+}-free solution. *Rest* denotes nonstimulated condition. Times indicate exposure to thapsigargin (*Thap*). *C,* NFAT1 movement to thapsigargin stimulation in the presence of 2 mM external Ca^{2+}. *D,* NFAT1 movement co-localizes with DAPI staining of the nucleus. *E,* nuclear movement of NFAT1 in response to thapsigargin is suppressed by a CRAC channel blocker (Synta compound, *upper panel*), cyclosporin A (*Cyclo. A*, *middle panel*), and antimycin A/oligomycin (*A/O, lower panel*). *F,* aggregate data from several cells for each condition is compared ($2Ca^{2+} = 4$ cells, $0Ca^{2+} = 5$ cells, *Synta,* cyclosporin A, and *A/O*, antimycin A and oligomycin = 4, 3, and 5 cells, respectively). The *y* axis represents the nuclear/cytosolic ratio of NFAT1-GFP, measured initially in nonstimulated cells and then after 40 min treatment with thapsigargin in external Ca^{2+} solution.

location in response to thapsigargin. Pretreatment with KN62 (10 μM), to block CaMKII, had little effect on NFAT movement in response to thapsigargin (after 20 min of stimulation, nuclear/cytoplasmic NFAT-GFP was 1.22 ± 0.03 for 5 control cells and 1.16 ± 0.03 in the presence of KN-62 for 5 cells; $p > 0.1$).

In many cell types, CRAC channel activity is controlled by mitochondria (19). In RBL-1 mast cells, mitochondrial depolarization reduces Ca^{2+} influx (16, 20) and therefore subsequent downstream Ca^{2+}-dependent responses (21). Consistent with this, mitochondrial depolarization following the combination of antimycin A and oligomycin reduced store-operated Ca^{2+} entry (the global Ca^{2+} rise upon readmission of external Ca^{2+} to cells treated with thapsigargin in Ca^{2+}-free solution was reduced by ~60%, data not shown) and suppressed NFAT1 movement to the nucleus (Fig. 1, *E* and *F*). These results complement recent studies in sensory neurons and T cells that found a prominent role for mitochondria in regulating NFAT movement into the nucleus in response to voltage-gated Ca^{2+} channel and CRAC channel activation (22, 23).

To obtain a better estimate of the kinetic relationship between Ca^{2+} entry through CRAC channels and NFAT1 movement, we stimulated cells with thapsigargin in Ca^{2+}-free solution to deplete the stores and, once cytoplasmic Ca^{2+} had returned to resting levels, we readmitted external Ca^{2+} (Fig. 2*A*) and measured NFAT1 movement to the nucleus as a function of the duration of Ca^{2+} influx. No resolvable movement occurred within 4 min of Ca^{2+} readmission, but migration was discernible after 8 min (Fig. 2*B*). Aggregate data from several cells are depicted in Fig. 2*C*. The relationship was best fitted by a sigmoidal function, yielding a lag phase of ~4 min followed by an increase in nuclear migration with time. The lag phase likely reflects NFAT dephosphorylation in the cytosol (Fig. 5), a process that precedes NFAT movement.

NFAT1 Movement Shows Short Term Memory—NFAT1 translocation to the nucleus did not correlate tightly with the time course of the cytoplasmic Ca^{2+} signal. Although cytoplasmic Ca^{2+} was elevated within 1 min of stimulation with thapsigargin (Fig. 1*A*), NFAT1 migration to the nucleus was not detectable until several minutes later (Fig. 1*C*). Furthermore, the Ca^{2+} signal in the presence of external Ca^{2+} decreased with time (Fig. 1*A*), due to Ca^{2+}-dependent inactivation of CRAC channels, yet NFAT1 movement continued. For example, there was little difference in cytoplasmic Ca^{2+} between 20 and 40 min of thapsigargin stimulation (Fig. 1*A*), yet NFAT1 movement increased over this time period (Fig. 1*C*). Hence, NFAT1 continues to migrate to the nucleus even after Ca^{2+} returns to basal levels, indicating a form of memory, as has been described previously (24). To obtain a more quantitative measure of this phenomenon, we applied a pulse of Ca^{2+} entry for 10 min and measured subsequent NFAT1 movement for a further 40 min. Stores were depleted following exposure to thapsigargin in Ca^{2+}-free solution, and then external Ca^{2+} was readmitted before cells were perfused with Ca^{2+}-free solution once more (Fig. 2*D*). The cytoplasmic Ca^{2+} signal because of Ca^{2+} influx fell rapidly upon exposure to Ca^{2+}-free solution (Fig. 2*D*), but NFAT1-GFP continued to migrate to the nucleus for several minutes (Fig. 2*E*). Kinetic analysis of the movement showed that NFAT continued to accumulate within the nucleus for 20 min after cytoplasmic Ca^{2+} had recovered to resting levels (Fig. 2*F*), indicating prominent short term memory.

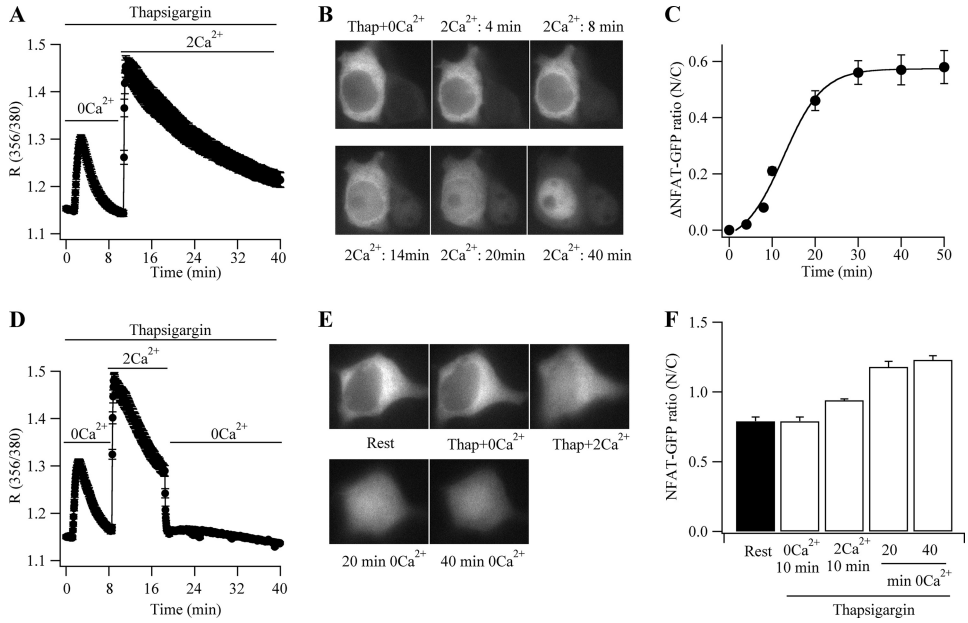

FIGURE 2. **Time course of NFAT1 movement following CRAC channel opening.** *A*, time course of the Ca^{2+} signal following readmission of external Ca^{2+} to cells with depleted stores is shown (average of 17 cells). *B*, NFAT1 movement into the nucleus is shown following Ca^{2+} readmission for different times. *C*, time course of NFAT1-GFP movement (average of five cells) is plotted against Ca^{2+} readmission time. The *y* axis shows the change in nuclear/cytoplasmic (*N/C*) ratio from the resting state. *D*, protocol evoking a pulse of Ca^{2+} entry is shown (average of 18 cells). *E*, NFAT1 movement is shown before and after Ca^{2+} removal. *F*, *histogram* summarizes aggregate data for the different conditions shown (four cells for each bar). *Thap.*, thapsigargin.

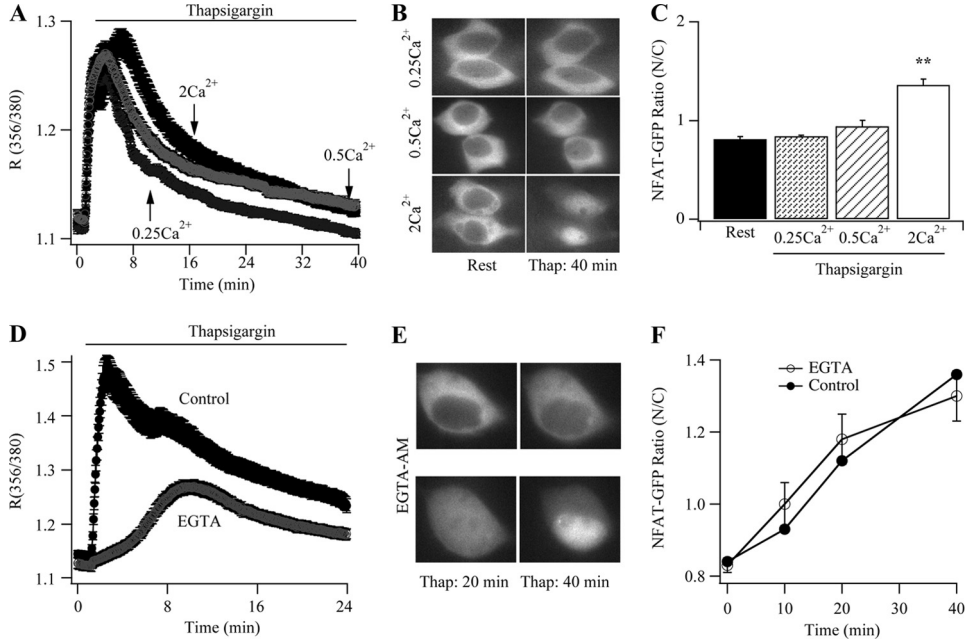

FIGURE 3. **Local Ca^{2+} signals drive NFAT1 migration.** *A*, Ca^{2+} signals following thapsigargin (*Thap.*) stimulation in different external Ca^{2+} concentrations (n = 18 for 2 Ca^{2+}, n = 23 for 0.5 Ca^{2+}, and n = 16 for 0.25 Ca^{2+}). *B*, NFAT1 movement in response to stimulation with thapsigargin in 0.25 mM (*upper panel*), 0.5 mM (*middle*), and 2 mM Ca^{2+} (*lower panel*). *C*, aggregate data for each condition is summarized (n is between 4 and 7 cells for each point). NFAT ratio is shown for 40 min stimulation. *D*, Ca^{2+} signals are compared between control cells (n = 17) and those preloaded with EGTA-AM (n = 19). *E*, NFAT1 movement in the presence of cytoplasmic EGTA. *F*, time course of NFAT1 movement is compared for control cells and those loaded with EGTA (n = 7 for each condition). *N/C*, nuclear/cytoplasmic ratio.

NFAT1 Movement and Local Ca^{2+} Influx—We designed experiments to explore whether NFAT1 movement was activated by local Ca^{2+} entry through CRAC channels. A hallmark of processes driven by Ca^{2+} microdomains is that they are much more sensitive to the Ca^{2+} flux through single channels than the bulk cytoplasmic Ca^{2+} rise (3). To manipulate the single channel Ca^{2+} current, we varied external Ca^{2+} concentration over the range 0.25–2 mM. The Ca^{2+} response in 0.25 mM external Ca^{2+} was significantly smaller than that in 2 mM Ca^{2+} (Fig. 3*A*) and was completely ineffective in driving NFAT1 movement to the nucleus (Fig. 3, *B* and *C*). Stimulation with thapsigargin in 0.5 mM external Ca^{2+} produced similar bulk Ca^{2+} signals to those seen in 2 mM Ca^{2+} (Fig. 3*A*). However, despite this, stimulation with thapsigargin in 0.5 mM Ca^{2+}

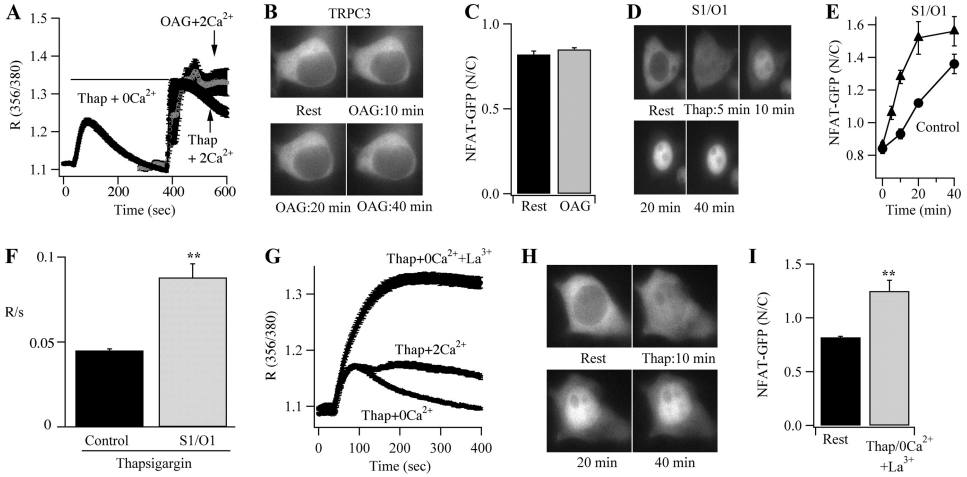

FIGURE 4. **NFAT1 movement is tightly coupled to CRAC channels.** *A*, Ca^{2+} signals evoked by CRAC channels and TRPC3 channels (activated by OAG) are compared. *B*, images show the lack of effect of OAG on NFAT1 movement. *C*, aggregate data are shown comparing the basal nuclear/cytoplasmic (*N/C*) NFAT ratio with that seen after 40 min of stimulation with OAG ($n = 16$ cells). *D*, images show the effect of overexpression of STIM1 and Orai1 (*S1/O1*) on NFAT movement. *E*, time course of NFAT movement is compared between control cells (with endogenous CRAC channel activity) and cells transfected with STIM1 and Orai1 ($n = 6–9$ cells for each condition). *F*, *histogram* compares the rate of rise of the Ca^{2+} signal, obtained upon readmission of external Ca^{2+} to cells with depleted stores, for the two conditions shown ($n = 16$ for control and $n = 11$ for *S1/O1*). *G*, inhibition of Ca^{2+} extrusion with 1 mM La^{3+} increases the size and prolongs the time course of the Ca^{2+} rise to thapsigargin (*Thap*) in Ca^{2+}-free external solution ($n = 21$ for $0Ca^{2+}$, $n = 20$ for $0Ca^{2+} + La^{3+}$, $n = 21$ for 2 Ca^{2+}). In these experiments, we used the low affinity dye Fura-5F because Fura-2 would have been saturated by the larger Ca^{2+} signal. *H*, images show NFAT1 movement following stimulation with thapsigargin in Ca^{2+}-free solution supplemented with La^{3+}. *I*, aggregate data are compared for the conditions shown ($n = 4$ cells).

failed to generate any significant movement of NFAT1 movement into the nucleus (Fig. 3, *B* and *C*).

A further prediction of dependence on Ca^{2+} microdomains is that a slow Ca^{2+} chelator such as EGTA should have little effect on NFAT1 movement in response to CRAC channel opening. Because of its slow on-rate for binding Ca^{2+}, EGTA has no impact on the extent of the Ca^{2+} microdomain within a few tens of nanometers of the CRAC channel pore (2, 3). We therefore loaded cells with EGTA (by incubation in 25 μM EGTA-AM for 45 min) and then stimulated them with thapsigargin in the presence of 2 mM Ca^{2+}. The bulk Ca^{2+} signal was substantially reduced in EGTA-loaded cells (Fig. 3*D*), as expected from an increase in cytoplasmic Ca^{2+} buffering. However, NFAT1 migration was largely unaffected (Fig. 3, *E* and *F*).

NFAT1 Activation Is Tightly Coupled to CRAC Channels—We asked if NFAT1 could be activated by a generalized rise in subplasmalemmal Ca^{2+} or whether it was tightly coupled to CRAC channels. A prediction of the former mechanism is that other Ca^{2+}-permeable ion channels should be capable of activating NFAT1. We expressed TRPC3 channels, which are nonselective cation channels permeable to Ca^{2+} (25). Activation of these channels with the diacylglycerol analog 1-oleoyl-2-acetyl-*sn*-glycerol (OAG, 50 μM) evoked robust bulk Ca^{2+} signals that were similar in size to those generated following endogenous CRAC channel activation (Fig. 4*A*; OAG signals are shown in *gray*). However, NFAT1 failed to move to the nucleus upon activation of TRPC3 (Fig. 4*B*; aggregate data is shown in Fig. 4*C*). Nontransfected HEK293 cells failed to respond to OAG, confirming that the Ca^{2+} signals were indeed a consequence of TRPC3 expression (data not shown). NFAT1 movement out of the nucleus (using a protocol described in Fig. 5) was not accelerated by OAG exposure (data not shown), suggesting movement into the nucleus was not being masked by accelerated nuclear exit. Overexpression of Orai1 (with STIM1) increased NFAT1 migration significantly (Fig. 4, *D* and *E*), along with a faster rate of Ca^{2+} entry (Fig. 4*F*), compared with the corresponding rates with endogenous CRAC channel activity. Collectively, these results reveal that a generalized rise in subplasmalemmal Ca^{2+} is not sufficient for NFAT movement. Rather, local Ca^{2+} signals close to CRAC channels are critical.

Calculations estimate the local Ca^{2+} concentration near CRAC channels to be in the low micromolar range (3). One might therefore expect that if a large and sustained bulk increase in cytoplasmic Ca^{2+}, arising exclusively from Ca^{2+} release, raises subplasmalemmal Ca^{2+} to a similar extent, then this should also activate NFAT1 movement. To test this, we used a method described previously (7, 26, 27) that produces a large and prolonged Ca^{2+} signal through the combined exposure to thapsigargin in Ca^{2+}-free external solution (to prevent any Ca^{2+} entry) supplemented with La^{3+}. La^{3+} inhibits the plasma membrane Ca^{2+}ATPase pump, reducing Ca^{2+} extrusion across the plasma membrane. Stimulation with thapsigargin in the presence of Ca^{2+}-free solution containing 1 mM La^{3+} led to a robust and prolonged Ca^{2+} signal, considerably larger than that seen in the absence of La^{3+} or in response to thapsigargin in 2 mM Ca^{2+} (Fig. 4*G*), and this larger signal was associated with strong NFAT1 movement to the nucleus (Fig. 4, *H* and *I*). Hence, NFAT1 migration is not absolutely dependent on Ca^{2+} entry; Ca^{2+} release also drives movement provided it is of sufficient amplitude and duration.

Kinetic Features of NFAT1 Activation and Nuclear Dynamics—Accumulation of NFAT1 within the nucleus is a multistep process involving the following: (i) NFAT1 dephosphorylation in the cytoplasm by calcineurin; (ii) NFAT1 movement into the nucleus, and (iii) NFAT1 exit from the nucleus. We measured the kinetics of each of these steps following CRAC channel activation, to compare the Ca^{2+} signal with NFAT dynamics. NFAT dephosphorylation can be monitored by tracking the gel

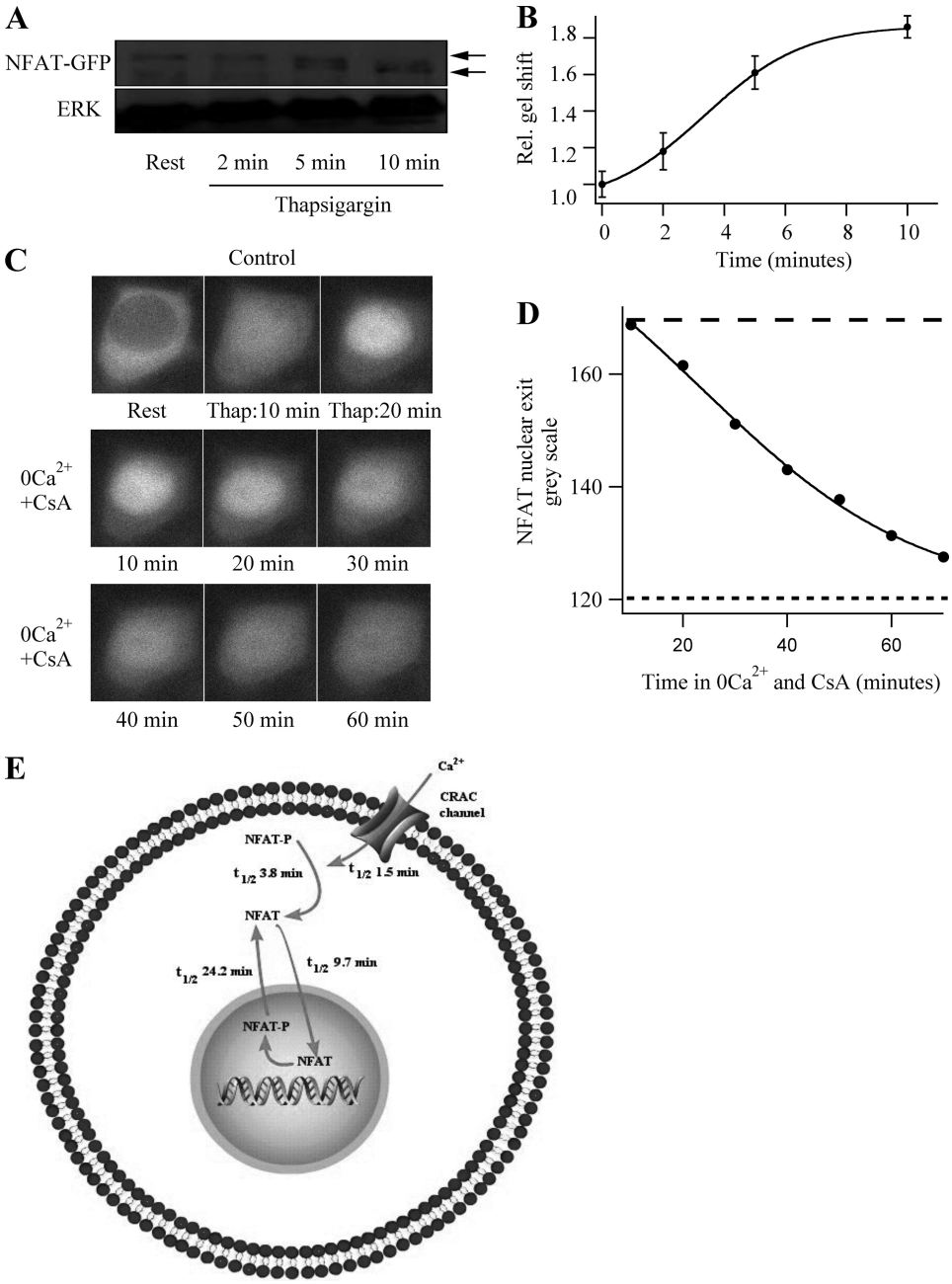

FIGURE 5. **Quantification of the kinetics of NFAT1 activation and movement into and out of the nucleus.** *A,* representative gel showing NFAT1 dephosphorylation (measured from the gel shift, as shown by the *two arrows*) following stimulation with thapsigargin. *B,* aggregate data from two independent gels is summarized. *C,* images show movement of NFAT out of nucleus after termination of Ca^{2+} entry together with block of calcineurin ($0Ca^{2+}$ + cyclosporin A (*CsA*)). Cells were stimulated with thapsigargin (*Thap*) for 20 min in the presence of external Ca^{2+} before Ca^{2+} entry was terminated. *D,* graph plots the migration of NFAT1 out of the nucleus as a function of time in Ca^{2+}-free solution ($n = 5$ cells). The *upper dashed line* shows the nuclear NFAT1-GFP fluorescence after 20 min stimulation with thapsigargin, and the *lower dashed line* indicates the absolute level of NFAT1-GFP fluorescence in the cytosol prior to stimulation (*rest*). The absolute levels of NFAT1-GFP (*gray scale*) were measured and not the ratio, because NFAT1 flux out of the nucleus was being evaluated, and *error bars* have been omitted for clarity. At 20 and 40 min for example, the absolute values were 161.5 ± 16.1 and 143.0 ± 11.7 (*E*). Schematic summarizes the kinetics (half-time ($t_{1/2}$) of the various steps that regulate NFAT1 movement into and out of the nucleus.

shift that occurs upon dephosphorylation of NFAT (Fig. 5*A*). As shown in Fig. 5*B*, dephosphorylation proceeded relatively rapidly, reaching completion within 10 min. This is in good agreement with previous studies that reported substantial dephosphorylation within 5 min (24, 28). To measure migration out of the nucleus, we initially triggered NFAT1-GFP movement into the nucleus by stimulation with thapsigargin in 2 mM external Ca^{2+} for 20 min and then suppressed Ca^{2+} influx by removing external Ca^{2+} and simultaneously inhibited calcineurin with cyclosporin A. NFAT migrated slowly out of the nucleus (Fig. 5*C*; aggregate data from several cells is summarized in Fig. 5*D*). The schematic in Fig. 5*E* summarizes the half-times for each of the key steps in NFAT1 dynamics. This is not a quantitative model and suffers from some limitations. First, NFAT1 movement has been measured at the single cell level, whereas the kinetics of cytoplasmic dephosphorylation was derived from

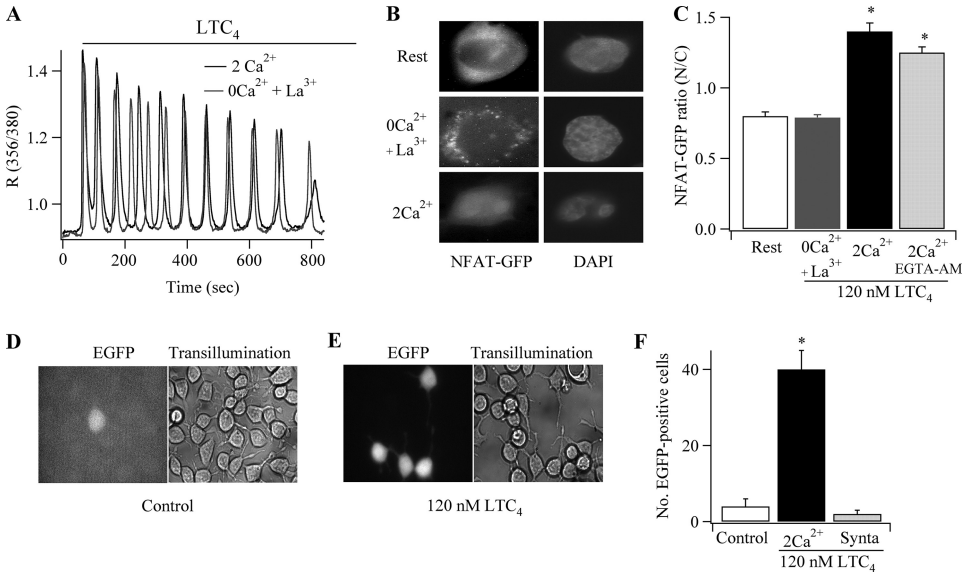

FIGURE 6. **Local Ca^{2+} entry evoked by an agonist drives NFAT1 movement.** *A,* stimulation of Fura-5F-loaded cells with 120 nM LTC_4 in the presence of external Ca^{2+} (*black trace*) or absence of external Ca^{2+} with 1 mM La^{3+} evokes Ca^{2+} oscillations of similar amplitude and frequency. *B,* images show distribution of NFAT1-GFP (*left panels*) and DAPI (*right panels*) for rest (nonstimulated), $0Ca^{2+} + La^{3+}$ (exposed to LTC_4 for 10 min), and $2Ca^{2+}$ (LTC_4 was applied for 10 min). *C,* aggregate data from several cells is shown. N/C, nuclear/cytoplasmic ratio. *D,* EGFP gene expression is compared between nonstimulated (control) cells and those exposed to 120 nM LTC_4 (40 min). *E, histogram* compares the number of EGFP-positive cells for the different conditions. Data are the aggregate from six fields of view from three coverslips each.

Western blots and is therefore an ensemble of thousands of cells. Individual cellular dephosphorylation kinetics, which could vary significantly between cells, cannot be related to NFAT1 movement in the same cell. Second, NFAT1 exit from the nucleus is not a true unidirectional measurement because it occurs in the presence of NFAT1 migration into the nucleus, although precautions were taken to abolish the latter process by abolishing Ca^{2+} flux through CRAC channels together with inhibition of calcineurin. The presence of cyclosporin A prevented the continued movement of NFAT-GFP upon removal of external Ca^{2+} that was seen in experiments of the type described in Fig. 2 (data not shown). Third, we were unable to separate the two steps involved in NFAT1 nuclear exit, namely nuclear phosphorylation and efflux. The $t½$ of 24.2 min in Fig. 5 combines both together. Finally, it is conceivable that the GFP tag on NFAT1 impairs its transport into and out of the nucleus, and to different extents. Nuclear import and export of an NFAT-GFP construct in sensory neurons in response to voltage-gated Ca^{2+} channel activity are both significantly faster (~2- and 5-fold, respectively) than the values we report here, suggesting the presence of the GFP tag *per se* might not compromise NFAT dynamics significantly. Notwithstanding these issues, the model reveals NFAT migration out of the nucleus as the step with the slowest kinetics.

Local Ca^{2+} Entry Evoked by Agonist Drives NFAT1 to the Nucleus—To examine whether local Ca^{2+} entry through CRAC channels stimulates NFAT1 movement to the nucleus in response to physiological levels of agonist, we expressed NFAT1-GFP in a mast cell line and stimulated endogenous cysteinyl leukotriene receptors with a sub-maximal concentration (120 nM) of LTC_4. This concentration of agonist triggers repetitive Ca^{2+} oscillations in the presence of external Ca^{2+} (Fig. 6*A*, *black trace*) or in the absence of external Ca^{2+} provided La^{3+} is present extracellularly to inhibit Ca^{2+} extrusion via the plasma membrane Ca^{2+}ATPase pump (Fig. 6*A*, *gray traces*) (7). In the former case, Ca^{2+} entry through CRAC channels refills the stores and sustains the oscillatory response. In the presence of La^{3+}, Ca^{2+} released from the endoplasmic reticulum is pumped back into the stores to support repetitive Ca^{2+} release. The oscillations have identical amplitudes and frequencies, but the underlying spatial Ca^{2+} gradients are different (7). Only those oscillations that occur in the presence of external Ca^{2+} generate local Ca^{2+} signals near open CRAC channels, which selectively couple to gene expression (7). Stimulation with LTC_4 in the presence of 0 Ca^{2+} plus La^{3+} consistently failed to trigger an increase in NFAT1 migration to the nucleus (Fig. 6, *B* and *C*). However, significant movement occurred when the same dose of agonist was applied in the presence of external Ca^{2+}, despite evoking Ca^{2+} oscillations of the same amplitude and frequency. Hence, local Ca^{2+} entry through CRAC channels drives NFAT1 migration to the nucleus when low doses of a physiological agonist are used. Consistent with this, loading the cytoplasm with the slow Ca^{2+} chelator EGTA (through preincubation with EGTA-AM) failed to prevent NFAT1 movement into the nucleus following stimulation with LTC_4 (Fig. 6*C*).

Local Ca^{2+} Entry by Agonist Drives NFAT-dependent Gene Expression—To examine whether NFAT1 migration to the nucleus in response to Ca^{2+} microdomains near CRAC channels led to gene expression, we transfected cells with an EGFP plasmid driven by an NFAT promoter. Whereas very few cells expressed EGFP in the absence of stimulation (Fig. 6, *D* and *F*), exposure to 120 nM LTC_4 (for 40 min) led to a significant increase in the number of EGFP-positive cells (Fig. 6, *E* and *F*). Blocking CRAC channels with the Synta compound (5 μM; 10 min pretreatment) completely abolished gene expression in response to LTC_4 (Fig. 6*F*). As we have shown recently, LTC_4 still evokes Ca^{2+} oscillations in the presence of CRAC channel

blockers (7). However, these oscillations are similar to those obtained in Ca^{2+}-free solution and run down more quickly than those obtained in 2 mM external Ca^{2+} in the absence of CRAC channel blockers. Whereas Ca^{2+} oscillations to 120 nM LTC_4 in 2 mM Ca^{2+} continue for 10 min of stimulation, those in the presence of CRAC channel blockers are lost after ~7 min (supplemental Fig. 1). Nevertheless, 4 ± 1 robust Ca^{2+} oscillations occurred in the presence of the Synta compound, yet these failed to evoke any detectable gene expression. Our attempts to evoke sustained Ca^{2+} oscillations by stimulating with LTC_4 in Ca^{2+}-free solution supplemented with 1 mM La^{3+} were thwarted by the fact that La^{3+} was precipitated in the culture medium.

Concluding Remarks—As with activation of NFAT in neurons following the opening of L-type Ca^{2+} channels, several independent pieces of evidence reveal that NFAT1 activation is acutely tuned to Ca^{2+} microdomains near open CRAC channels in the nonexcitable cells we have examined. First, NFAT1 migration to the nucleus was minimal when cells were challenged in reduced external Ca^{2+} (0.5 mM), despite global Ca^{2+} being similar to that obtained in 2 mM Ca^{2+}. Second, the slow Ca^{2+} chelator EGTA had little effect on NFAT1 movement despite reducing bulk Ca^{2+}. Third, activation of other Ca^{2+}-permeable pathways, including TRPC3 channels, failed to elicit NFAT1 movement despite a similar rise in bulk Ca^{2+} to that evoked by CRAC channel opening. This latter result reveals that not all Ca^{2+}-permeable pathways are equally effective in activating NFAT1, despite raising bulk Ca^{2+} to similar extents. By contrast, overexpression of Orai1 greatly accelerated NFAT1 movement into the nucleus. Hence the level of CRAC channel expression will impact significantly on the rate and extent of NFAT1 movement. How can NFAT1 be tightly linked to local Ca^{2+} signals? The Ca^{2+} sensor in the NFAT activation pathway must presumably be co-localized with the CRAC channel. The sensor is probably calmodulin, which, when occupied by Ca^{2+}, activates calcineurin. Recent work has revealed that calmodulin can bind to the amino terminus of Orai1 (29), providing a mechanism whereby the sensor for the NFAT1 pathway can detect local Ca^{2+} signals near CRAC channels. In hippocampal neurons, calcineurin is held close to the L-type Ca^{2+} channel through AKAP79/150 (9). It will be interesting to see whether such scaffolding proteins play a similar role in nonexcitable cells.

Although our findings reveal an important role for local Ca^{2+} entry through CRAC channels in driving NFAT movement to the nucleus and subsequent gene expression, they do not rule out a role for global Ca^{2+} under certain conditions. Our experiments using stimulation with thapsigargin, 0 Ca^{2+}/La^{3+} demonstrate global Ca^{2+} can drive NFAT movement, provided it is high enough to elevate subplasmalemmal Ca^{2+} near CRAC channels and thus occupy the Ca^{2+} sensor. It has been established that a sustained Ca^{2+} rise of more than ~400 nM for ~2 h is required for NFAT-dependent expression of genes that commit T cells to activation (30, 31). Although it is not clear whether NFAT activation is dependent on local or global Ca^{2+} signals in these cells, it is interesting to note that the commonly used methods for raising Ca^{2+} in such experiments involve either activation of the T cell receptor or application of the ionophore ionomycin. Both approaches open CRAC channels and therefore will produce local Ca^{2+} signals below the membrane that will diverge significantly from bulk Ca^{2+} measurements. These spatial gradients will be accentuated by the substantial increase in plasma membrane Ca^{2+}ATPase pump activity that occurs following CRAC channel opening in T cells (32). It is noteworthy that stimulation with thapsigargin in 0.5 mM Ca^{2+} elicited a similar bulk Ca^{2+} rise and of similar duration to that triggered by thapsigargin in 2 mM Ca^{2+}, but only the latter led to NFAT1 movement. Hence, the duration of the bulk Ca^{2+} rise does not seem as important as the properties of the local Ca^{2+} signal in activating NFAT1, at least under our experimental conditions.

Local Ca^{2+} signals arising from focal release of Ca^{2+} into the nucleus by perinuclear inositol trisphosphate receptors have been reported to activate the calcineurin/NFAT pathway in atrial myocytes (33). NFAT activation can therefore occur in response to local Ca^{2+} gradients arising from either Ca^{2+} release directly into the nucleus or through Ca^{2+} entry via plasma membrane CRAC channels. It is conceivable that these two components reinforce one another in response to physiological stimuli. Alternatively, they could operate independently, enabling selective activation of the NFAT pathway through recruitment of different phases of the Ca^{2+} signal.

At the immunological synapse, which forms on a T cell membrane where it apposes an antigen-presenting cell, receptors, signaling molecules, and Orai1 and STIM1 can accumulate (34). It is tempting to speculate that local Ca^{2+} signals through CRAC channels confined to the immunological synapse might selectively drive NFAT activation and subsequent NFAT-dependent gene expression.

The marked temporal dissociation between the time course of the cytoplasmic Ca^{2+} rise and NFAT1 migration to the nucleus reveals a form of short term memory that maintains gene expression long after the Ca^{2+} stimulus has been removed. A pulse of Ca^{2+} influx for ~10 min was sufficient for NFAT1 to continue to accumulate in the nucleus even 20 min later. Similar temporal uncoupling between the Ca^{2+} signal and NFAT movement has been seen in cultured hippocampal neurons, where a depolarization for a few minutes was sufficient for continued NFAT accumulation within the nucleus (8, 9). Such temporal uncoupling between the Ca^{2+} signal and NFAT1 activation provides a mechanism for sustaining Ca^{2+}-dependent nuclear events without the obvious disadvantages that arise from a protracted bulk Ca^{2+} signal (35, 36). NFAT-dependent gene expression can be maintained by repetitive cytoplasmic Ca^{2+} oscillations (37), with a periodicity of <400 s in T lymphocytes (38). NFAT movement out of the nucleus in studies on T cell populations is considerably slower than the decay of the Ca^{2+} signal, with almost 50% of the NFAT pool remaining within the nucleus 10 min after cessation of the Ca^{2+} spike (39). This is in good agreement with our single cell analysis and suggests each pulse of Ca^{2+} tops up the nuclear NFAT pool sufficiently to maintain gene expression.

Finally, our kinetic analysis of the three main stages involved in NFAT1 nuclear accumulation reveals that NFAT1 activation (arising from cytoplasmic dephosphorylation) and migration into the nucleus are both considerably faster (~10- and 3-fold,

respectively) than NFAT movement out of the nucleus. Nuclear export of NFAT in hippocampal neurons is also relatively slow, with a reported half-time of ~10 min (8). Our results establish that the slow off-rate for NFAT1 (exodus from the nucleus) is a major factor in determining its nuclear buildup and thereby gene expression. Slow off-rates in Ca^{2+}-dependent signaling might therefore be an effective general strategy for ensuring long lasting responses following termination of the Ca^{2+} trigger.

REFERENCES

1. Berridge, M. J., Bootman, M. D., and Roderick, H. L. (2003) *Nat. Rev. Mol. Cell Biol.* **4,** 517–529
2. Neher, E. (1998) *Neuron* **20,** 389–399
3. Parekh, A. B. (2008) *J. Physiol.* **586,** 3043–3054
4. Rizzuto, R., and Pozzan, T. (2006) *Physiol. Rev.* **86,** 369–408
5. Dolmetsch, R. E., Pajvani, U., Fife, K., Spotts, J. M., and Greenberg, M. E. (2001) *Science* **294,** 333–339
6. Deisseroth, K., Heist, E. K., and Tsien, R. W. (1998) *Nature* **392,** 198–202
7. Di Capite, J., Ng, S. W., and Parekh, A. B. (2009) *Curr. Biol.* **19,** 853–858
8. Graef, I. A., Mermelstein, P. G., Stankunas, K., Neilson, J. R., Deisseroth, K., Tsien, R. W., and Crabtree, G. R. (1999) *Nature* **401,** 703–708
9. Oliveria, S. F., Dell'Acqua, M. L., and Sather, W. A. (2007) *Neuron* **55,** 261–275
10. Hogan, P. G., Chen, L., Nardone, J., and Rao, A. (2003) *Genes Dev.* **17,** 2205–2232
11. Hoth, M., and Penner, R. (1992) *Nature* **355,** 353–356
12. Parekh, A. B., and Putney, J. W., Jr. (2005) *Physiol. Rev.* **85,** 757–810
13. Clipstone, N. A., and Crabtree, G. R. (1992) *Nature* **357,** 695–697
14. Hogan, P. G., Lewis, R. S., and Rao, A. (2010) *Annu. Rev. Immunol.* **28,** 491–533
15. Feske, S., Gwack, Y., Prakriya, M., Srikanth, S., Puppel, S. H., Tanasa, B., Hogan, P. G., Lewis, R. S., Daly, M., and Rao, A. (2006) *Nature* **441,** 179–185
16. Glitsch, M. D., Bakowski, D., and Parekh, A. B. (2002) *EMBO J.* **21,** 6744–6754
17. Glitsch, M. D., Bakowski, D., and Parekh, A. B. (2002) *J. Physiol.* **539,** 93–106
18. Ng, S. W., di Capite, J., Singaravelu, K., and Parekh, A. B. (2008) *J. Biol. Chem.* **283,** 31348–31355
19. Parekh, A. B. (2008) *Cell Calcium* **44,** 6–13
20. Gilabert, J. A., and Parekh, A. B. (2000) *EMBO J.* **19,** 6401–6407
21. Chang, W. C., and Parekh, A. B. (2004) *J. Biol. Chem.* **279,** 29994–29999
22. Kim, M. S., and Usachev, Y. M. (2009) *J. Neurosci.* **29,** 12101–12114
23. Hoth, M., Button, D. C., and Lewis, R. S. (2000) *Proc. Natl. Acad. Sci. U.S.A.* **97,** 10607–10612
24. Tomida, T., Hirose, K., Takizawa, A., Shibasaki, F., and Iino, M. (2003) *EMBO J.* **22,** 3825–3832
25. Trebak, M., St. J. Bird, G., McKay, R. R., Birnbaumer, L., and Putney, J. W., Jr. (2003) *J. Biol. Chem.* **278,** 16244–16252
26. Chang, W. C., Di Capite, J., Singaravelu, K., Nelson, C., Halse, V., and Parekh, A. B. (2008) *J. Biol. Chem.* **283,** 4622–4631
27. Bird, G. S., and Putney, J. W., Jr. (2005) *J. Physiol.* **562,** 697–706
28. Shaw, K. T., Ho, A. M., Raghavan, A., Kim, J., Jain, J., Park, J., Sharma, S., Rao, A., and Hogan, P. G. (1995) *Proc. Natl. Acad. Sci. U.S.A.* **92,** 11205–11209
29. Mullins, F. M., Park, C. Y., Dolmetsch, R. E., and Lewis, R. S. (2009) *Proc. Natl. Acad. Sci. U.S.A.* **106,** 15495–15500
30. Negulescu, P. A., Shastri, N., and Cahalan, M. D. (1994) *Proc. Natl. Acad. Sci. U.S.A.* **91,** 2873–2877
31. Lewis, R. S. (2001) *Annu. Rev. Immunol.* **19,** 497–521
32. Bautista, D. M., and Lewis, R. S. (2004) *J. Physiol.* **556,** 805–817
33. Higazi, D. R., Fearnley, C. J., Drawnel, F. M., Talasila, A., Corps, E. M., Ritter, O., McDonald, F., Mikoshiba, K., Bootman, M. D., and Roderick, H. L. (2009) *Mol. Cell* **33,** 472–482
34. Kummerow, C., Junker, C., Kruse, K., Rieger, H., Quintana, A., and Hoth, M. (2009) *Immunol. Rev.* **231,** 132–147
35. Petersen, O. H., and Tepikin, A. V. (2008) *Annu. Rev. Physiol.* **70,** 273–299
36. Parekh, A. B. (2000) *Proc. Natl. Acad. Sci. U.S.A.* **97,** 12933–12934
37. Li, W., Llopis, J., Whitney, M., Zlokarnik, G., and Tsien, R. Y. (1998) *Nature* **392,** 936–941
38. Dolmetsch, R. E., Xu, K., and Lewis, R. S. (1998) *Nature* **392,** 933–936
39. Dolmetsch, R. E., Lewis, R. S., Goodnow, C. C., and Healy, J. I. (1997) *Nature* **386,** 855–858